



HAL
open science

Hemolytic anemia and alterations in hepatic iron metabolism in aged mice lacking Cu,Zn-superoxide dismutase

Rafal Radoslaw Starzyński, François Canonne-Hergaux, Alexandra Willemetz, Mikolaj Antoni Gralak, Jaroslaw Woliński, Agnieszka Styś, Jaroslaw Olszak, Pawel Lipiński

► To cite this version:

Rafal Radoslaw Starzyński, François Canonne-Hergaux, Alexandra Willemetz, Mikolaj Antoni Gralak, Jaroslaw Woliński, et al.. Hemolytic anemia and alterations in hepatic iron metabolism in aged mice lacking Cu,Zn-superoxide dismutase. *Biochemical Journal*, 2009, 420 (3), pp.383-390. 10.1042/BJ20082137 . hal-00479120

HAL Id: hal-00479120

<https://hal.science/hal-00479120v1>

Submitted on 30 Apr 2010

HAL is a multi-disciplinary open access archive for the deposit and dissemination of scientific research documents, whether they are published or not. The documents may come from teaching and research institutions in France or abroad, or from public or private research centers.

L'archive ouverte pluridisciplinaire **HAL**, est destinée au dépôt et à la diffusion de documents scientifiques de niveau recherche, publiés ou non, émanant des établissements d'enseignement et de recherche français ou étrangers, des laboratoires publics ou privés.

Hemolytic anemia and alterations in hepatic iron metabolism in aged mice lacking Cu,Zn-superoxide dismutase

Rafał R. Starzyński*, François Canonne-Hergaux†, Alexandra Willemetz†, Mikołaj A. Gralak‡, Jarosław Woliński§, Agnieszka Styś*, Jarosław Olszak* and Paweł Lipiński*

*Department of Molecular Biology, Institute of Genetics and Animal Breeding, Polish Academy of Sciences, Jastrzębiec, 05-552 Wólka Kosowska, Poland

†Institut de Chimie des Substances Naturelles, CNRS, 91190 Gif-sur-Yvette, France

‡Department of Physiological Sciences, Warsaw University of Life Sciences, 02-776 Warsaw, Poland

§The Kielanowski Institute of Animal Physiology and Nutrition, Polish Academy of Sciences, 05-110 Jabłonna, Poland

Corresponding author: Paweł Lipiński, Department of Molecular Biology, Institute of Genetics and Animal Breeding, Polish Academy of Sciences, Jastrzębiec, ul. Postępu 1, 05-552 Wólka Kosowska, Poland. Tel: (48 22) 7561711. Fax: (48 22) 7561699; E-mail: p.lipinski@ighz.pl

Short title: SOD1 deficiency, hemolytic anemia and iron metabolism

SYNOPSIS

The continuous recycling of heme iron following phagocytosis and catabolism of senescent and damaged red blood cells by macrophages is a crucial process in the maintenance of systemic iron homeostasis. However, little is known about macrophage iron handling in hemolytic states resulting from a deficiency in antioxidant defenses. Our observations indicate that recently described [Iuchi Y, Okada F, Onuma K, Onoda T, Asao H, Kobayashi M, Fuji J. *Biochem. J.* (2007) **402**, 219-227] the chronic but moderate regenerative hemolytic anemia of old superoxide dismutase 1 (SOD1) knockout mice is associated with red blood cells modifications and sensitivity to both intra- and extravascular hemolysis. We have then characterized the molecular pathways of iron turnover in the liver of SOD1-deficient mice. Despite iron accumulation in liver macrophages namely Kupffer cells, we did not measure any significant change in non-heme liver iron. Interestingly in Kupffer cells, expression of the rate-limiting enzyme in heme degradation, the heme oxygenase-1 and expression of the iron exporter ferroportin were both upregulated whereas hepcidin mRNA level in the liver was decreased in *SOD1*^{-/-} mice. These results suggest that concerted changes in the hepatic expression of iron- and heme-related genes in response to hemolytic anemia in *SOD1*^{-/-} mice act to reduce toxic iron accumulation in the liver and respond to the needs of erythropoiesis.

Key words: erythrophagocytosis, iron, hemolysis, heme oxygenase, Kupffer cells, superoxide dismutase 1,

INTRODUCTION

Reactive oxygen species (ROS) are by-products of normal aerobic metabolism. Several antioxidant systems exist in cells to provide protection against ROS toxicity. The principal defense against the toxicity of superoxide ($O_2^{\cdot-}$), released mainly into the cytosol [1], is superoxide dismutase 1 (SOD1, Cu,Zn-SOD). Surprisingly, despite this crucial protective role, homozygous mutant mice lacking SOD1 are viable and phenotypically normal [2-4].

Permanent oxidative stress occurring due to elevated ROS later in life is an important mechanism in the pathogenesis of ageing [5]. In older mice, SOD1 deficiency results in an increased incidence of pathological changes [6-8]. In consequence, the lifespan of KO SOD1 mice is reduced by about 30% [3,4].

Mice with genetic SOD1 deficiency have been extensively used as an experimental animal model to explore SOD1 dysfunction-related pathologies [6,8,9]. With regard to hematological disorders, the critical role of alterations in redox state due to SOD1 deficiency has been reported in hemolytic anemia (HA) occurring in *SOD1*^{-/-} mice [10], as well as in the impairment of hematopoietic cell development in the mouse model of Fanconi anemia [11].

In this study we examined the consequences of HA in 1-year-old mice lacking Cu,Zn-SOD1 activity, focusing on alterations in their hepatic iron metabolism. Our data clearly indicate that the enhanced destruction and accelerated removal of RBC from the circulation of old *SOD1*^{-/-} mice induce substantial changes in the expression of genes involved in heme and iron homeostasis. Our results establish a new link between oxidative stress due to the combined effects of SOD1 deficiency and age-dependent changes in redox state and the regulation of iron metabolism at the systemic level.

EXPERIMENTAL

Animals

Mice homozygous for the non-functional *SOD1* allele, and control mice homozygous for the wild-type *SOD1* allele (wt) were used in experiments at the age of 1 year. A breeder pair of mice (strain B6;129S7-*SOD1*^{tm1Leb}) heterozygous for a *SOD1*^{tm1Leb} targeted mutation [3] were provided by The Jackson Laboratory (Bar Harbor, ME). The 3rd Local Ethical Commission approved all experimental procedures involving animals. (permission no. 46/2006).

Analysis of RBC and serum iron parameters

Blood was drawn from mice by direct cardiac puncture immediately after death and was treated with heparin. RBC and reticulocytes counts, and cell parameters as well as serum iron were determined using an automated Sysmex F-820 Analyzer. Serum transferrin was measured at the Laboratory of Biochemistry at the Institut Federatif de Recherche 02, CHU Bichat-Claude Bernard (Paris, France).

Real-time quantitative RT (reverse transcriptase)-Polymerase Chain Reaction

Hepatic ferroportin, hepcidin, CD91, CD163 mRNA levels were measured by real-time quantitative PCR method as described previously [12]. Real-time quantitative RT-PCR of cDNAs derived from specific transcripts was performed in a Light Cycler (Roche Diagnostics, Mannheim, Germany) using the respective pairs of oligonucleotide primers indicated in supplementary data (Table 1). For data analysis, Light Cycler 3.5 Software was used. Expression was quantified relative to that of a control transcript encoding glyceraldehyde-3-phosphate dehydrogenase (GAPDH).

Western Blot analysis

Fifty micrograms of liver cytosolic extracts (for ferritin (Ft) subunit detection) or 100 µg of liver membrane extracts [for heme oxygenase-1 (HO-1) and ferroportin (Fpn) detection] were resolved on 14% and 10% SDS-polyacrylamide gels, respectively. To determine plasma haptoglobin (Hp) and hemopexin (Hx) levels, samples were separated on 10% SDS-polyacrylamide gels. Resolved proteins were electroblotted onto Hybond-ECL nitrocellulose membranes (Amersham Life Sciences, Little Chalfont, UK). The membranes were initially blocked by gentle agitation in TBST (0.15% Tween 20 in Tris-buffered saline) containing 5% fat-free powdered milk for 1 hour at room temperature (RT) followed by overnight incubation at 4°C with primary antibodies: rabbit antisera raised against recombinant mouse H- and L-ferritin (H- and L-Ft; kindly provided by Dr. P. Santambrogio, Milan, Italy), rabbit polyclonal antibody raised against rat liver HO-1 (StressGen, Canada), rabbit antibody raised against mouse Fpn [13], chicken antibody raised against human Hp (USBiological, Swampscott, MA), and goat antiserum raised against human Hx (kindly provided by Dr. E. Tolosano, University of Turin, Italy). Membranes were then washed and incubated with peroxidase-conjugated anti-rabbit, anti-chicken or anti-goat secondary antibodies (Santa Cruz Biotechnology, Santa Cruz, CA) for 1 hour at room temperature. Immunoreactive bands were detected using the ECL Plus enhanced chemiluminescence Western blotting detection system (Amersham Life Sciences). Quantification was performed relative to actin detected using a specific antibody (Santa Cruz Biotechnology, Santa Cruz, CA).

Immunohistofluorescence

Mouse livers were fixed in Bouin's for 72 hours at 20°C and then embedded in paraffin for sectioning. After mounting on glass slides, 5 µm sections were processed for immunofluorescence. The sections were first counterstained with 0.1% methylene blue in PBS and mounted in Permount. The sections were then incubated in a blocking solution for 45 minutes at RT. Incubation with primary antibodies was performed in a humid chamber at RT for 16 hours using the following dilutions in blocking solution: anti-Fpn, 1/75 and anti-HO-1, 1/100. After three washes with PBS/0.5% BSA, the sections were incubated for 1 hour at RT with a goat anti-rabbit-Alexa 488-conjugated secondary antibody (Molecular Probes) diluted 1/200 in blocking solution. After washing, the slides were coverslipped with anti-fading mounting reagent (Prolong Antifade kit P-7481, Molecular Probes) and examined for immunofluorescence.

Quantitative hepatic non-heme iron measurement and hepatic iron staining

Hepatic non-heme iron content was determined by acid digestion of liver samples at 65°C for 20 hours followed by colorimetric measurement of the absorbance of iron-ferrozine complex at 560 nm as described previously [14]. Deparaffinized liver sections were stained with Prussian blue and counterstained with nuclear red using standard procedures.

FACS analysis of phosphatidylserine (PS) externalization

The presence of PS on the surface of mouse RBC membranes was assessed using Annexin V-FITC staining (Calbiochem) following the manufacturer's protocol. Stained cells were analyzed by flow-cytometry (FACS Calibur), and data were processed using CellQuest software (Becton Dickinson).

Erythrophagocytosis assay (EP)

EP assay was performed as described previously [15] using bone marrow-derived macrophages (BMDM) isolated from the femurs of *SOD1*^{-/+} mice and fresh RBCs obtained from 1-year-old mice of both *SOD1*^{-/-} and *SOD1*^{+/+} genotypes.

Heme content measurement

The heme content of formic acid-solubilized BMDM was determined spectrophotometrically at 398 nm using hemin standards prepared in formic acid and an extinction coefficient of $1.5 \times 10^5 \text{ M}^{-1} \text{ cm}^{-1}$ [16].

Statistical evaluation

Where suitable, one-way analysis of variance was applied to the data. The Scheffe test was used to estimate the significance of difference ($p < 0.05$) between means. All calculations were performed using Statgraphics Plus 6.0 software.

RESULTS

Moderate regenerative anemia in old *SOD1*^{-/-} mice

1-year-old *SOD1*^{-/-} mice show moderate anemia with reductions of about 25% in both erythrocyte number and hemoglobin (Hb) concentration, and a reduction of about 14% in the hematocrit value (Table 1). Values for the mean cell Hb concentration were unchanged, which together with normal levels of serum iron (Fig 1A) and transferrin (Fig 1B) may suggest that the anemia in *SOD1*^{-/-} animals is not associated with iron deficiency. The raised number of peripheral reticulocytes in *SOD1*^{-/-} mice (Fig 1C) as well as the increased spleen index values (Fig 1D) indicate that the anemia in *SOD1*^{-/-} mice is regenerative.

Hemoglobin and heme scavenging systems in *SOD1*^{-/-} mice

The findings obtained by Iuchi et al. [10] indicate that *SOD1*^{-/-} RBC are prone to hemolysis due to oxidative damage. Therefore, we attempted first to identify hallmarks of intravascular hemolysis. We measured plasma levels of haptoglobin (Hp) and hemopexin (Hx), two glycoproteins involved in the clearance of Hb and heme, respectively, from the blood stream. When Hb and hem are released from ruptured erythrocytes they are instantly bound by Hp and Hx and form Hp-Hb and Hx-heme high affinity complexes [17]. These complexes are then rapidly taken up from circulation by CD163 [18] and CD91 [19] receptors present on tissue macrophages and hepatocytes. The rationale for measuring Hp and Hx in the plasma is that CD163 and CD91 receptors have no measurable affinity for free Hp or Hx. Thus, specific recognition of Hp-Hb and Hx-heme complexes by CD163 and CD91 explains the decrease in Hp or Hx concentration in the plasma during accelerated hemolysis [19, 20]. Indeed, we found that the Hp level in plasma is strongly decreased in *SOD1*^{-/-} mice (Fig 2A). Surprisingly, higher plasma concentrations of Hx were detected in these animals compared with wt littermates. Considering the divergent patterns of Hp and Hx protein abundance in the plasma of *SOD1*-deficient mice, we analyzed the expression the *Hp1* and *Hx* genes in the liver, the major site of Hp and Hx synthesis [17]. The results shown in Fig 2B indicate that Hp as well as Hx mRNAs are markedly upregulated. We also measured expression of CD163 and CD91 transcripts in the liver, coding for receptors of Hp-Hb and Hx-heme complexes, respectively [18,19]. Levels of CD163 mRNA showed no differences between *SOD1*^{-/-} and *SOD1*^{+/+} mice, but the abundance of CD91 mRNA was significantly lower in *SOD1*-deficient mice (Fig 2C).

Indices of extravascular hemolysis in *SOD1*-deficient mice

To investigate the susceptibility of RBC to be removed from the circulation by erythrophagocytosis (EP), as a potential mechanism underlying hemolytic anemia, we evaluated the presence of phosphatidylserine (PS) externalized on the membranes of circulating erythrocytes. Flow-cytometry detection of externalized PS clearly showed a more than 3-fold increase in the percentage of PS-positive *SOD1*^{-/-} RBC when compared with wt

erythrocytes (Fig 3A). In artificially aged RBC [15], the proportion of PS translocated to the cell surface was significantly greater than the values found for *SOD1*^{-/-} and *SOD1*^{+/+} RBC. We next used an EP assay to examine the correlation between the levels of externalized PS with the heme content in *SOD1*^{-/-} BMDM after phagocytosis of RBC of the two genotypes. As expected, the heme content in BMDM after incubation with *SOD1*^{-/-} RBC was significantly greater than after incubation with wt RBC (Fig 3B) indicating that *SOD1*^{-/-} RBC are more readily phagocytosed than *SOD1*^{+/+} RBC.

Increase in hepatic heme oxygenase-1 (HO-1) expression in *SOD1*^{-/-} mice

To better understand the role of HO-1 during accelerated hemolysis, we analysed its expression in the liver, at both mRNA and protein levels (Fig 4). Levels of HO-1 mRNA were increased about 3-fold in *SOD1*^{-/-} mice compared with wt littermates (Fig 4A), and HO-1 protein levels assessed by both Western blotting (Fig 4B) and immunofluorescence (Fig 4C) were similarly elevated. Interestingly, HO-1 expression in liver was mostly detected in *SOD1*^{-/-} Kupffer cells (KC) in accordance to its known high expression in phagocytes. In contrast to wt mice, Hb autofluorescence was strongly present in liver sections from anemic *SOD1*^{-/-} mice (Fig 4D). Interestingly, fluorescence analysis of HO-1 (green) with Hb (red) showed partial co-localization in sections of liver from *SOD1*^{-/-} mice (Fig 4E).

Hepatic iron status in hemolytic *SOD1*^{-/-} mice

Massive iron accumulation in tissues is one of the characteristic metabolic features of acute hemolytic anemias of various etiologies [21]. We therefore examined whether this iron overload phenotype could be observed in hemolytic *SOD1*^{-/-} mice. Staining of non-heme iron in the liver showed iron accumulation in some *SOD1*^{-/-} liver macrophages (Fig 5A). On the other hand, no evident sign of global iron loading in hepatocytes was detected. Furthermore, we observed no significant change in non-heme iron content in the liver (Fig 5B). Accordingly, a significant decrease in L-ferritin protein (Fig 5C) in hepatic cytosolic extracts from *SOD1*^{-/-} mice was observed. The protein level of H-ferritin shows no difference between *SOD1*^{+/+} and *SOD1*^{-/-} mice.

Hepatic hepcidin (Hepc) mRNA and ferroportin (Fpn) protein levels are respectively decreased and increased in *SOD1*-deficient mice

We next studied the expression of Fpn, the only known iron exporter in mammalian cells. Western blotting of hepatic membrane extracts (Fig 6A) and immunofluorescence on histological liver sections (Fig 6B), showed that Fpn is expressed at low levels in the livers of *SOD1*^{+/+} mice. In contrast, Fpn expression was markedly enhanced in the livers of *SOD1*^{-/-} mice (Fig 6A and 6B). Microscope analysis of immunofluorescence staining on liver sections (Fig 6B) identified KC as the principal cell type of Fpn expression. Enlargement of immunofluorescent pictures also indicate the presence of RBC Hb autofluorescence in *SOD1*^{-/-} KC strongly positive for Fpn (see enlargement in Fig 6B). At the level of mRNA, we detected a slight but not significant change in Fpn mRNA expression between *SOD1*^{+/+} and *SOD1*^{-/-} animals (Fig 6C). Considering the established role of Hepc in the degradation of Fpn molecules [22], we then analyzed Hepc mRNA expression in mice of both genotypes and found that in *SOD1*^{-/-} mice, the expression of Hepc mRNA was decreased by about 70% (Fig 6D).

DISCUSSION

Here, we have investigated the consequences of oxidative stress due to the combined effects of SOD1 deficiency [4,6,10] and age-dependent alterations in redox state [4,6] on iron

homeostasis in old mice. Considering the well-known susceptibility of RBC to oxidative stress, and the importance of the liver in recycling heme iron, we focused our study on the peripheral erythrocyte-liver axis. Furthermore, analysis in the spleen of *SOD1*^{-/-} mice of markers of heme-iron recycling (HO-1, Fpn) and of the macrophage phagosome maturation (lysosome-associated membrane protein 1, Lamp1) indicate no major changes in heme-iron recycling in this tissue (supplementary data, Fig 1).

Our first observation concerning 1-year-old mice lacking Cu,Zn-SOD activity was reduction in the values of the main RBC parameters. A similar level of anemia has been reported in 40-week-old *SOD1*^{-/-} mice [10]. It has been proposed that oxidative stress is the major factor causing SOD1 deficiency anemia to qualify as a hemolytic anemia (HA) [10]. Because the mechanisms underlying HA are believed to rely on the destruction or accelerated removal of RBC from the circulation, we looked for evidence of intra- and extravascular hemolysis in old *SOD1*^{-/-} mice.

Hemoglobin (Hb) and heme are the most abundant iron compounds released into the plasma from ruptured RBC and they have been implicated in toxic effects [23]. Haptoglobin (Hp) and hemopexin (Hx), being scavengers of Hb and heme, respectively, are considered plasma-protective proteins against intravascular hemolysis [17]. The increased hepatic Hp gene expression and reduced plasma Hp protein level we observed in *SOD1*^{-/-} mice may reflect the induction of Hp synthesis in the liver, its release into the circulation followed by formation of the Hp-Hb complex, and its clearance by KC via CD163 [18]. Accordingly, the plasma level of Hp is usually reduced in hemeolytic states [17]. With regard to Hx, the increased levels found in the plasma of *SOD1*^{-/-} mice could be due to the fact that the amount consumed by moderate hemolysis is outweighed by its enhanced production as a result of inflammation in the liver. Furthermore, plasma Hx level starts to decrease when the Hb-binding capacity of Hp is exceeded [24]. Finally, low hepatic expression of CD91 mRNA (suggesting low protein expression) may also explain the high levels of Hx detected in the plasma of *SOD1*^{-/-} mice. In support of a role for enhanced extravascular hemolysis, i.e., accelerated erythrophagocytosis (EP), in HA in mice lacking SOD1, we observed the presence of RBC Hb autofluorescence in liver macrophages attesting of the high EP activity of these cells although Hb autofluorescence signal may also derive from internalized Hp-Hb complexes. We also demonstrated marked externalization of phosphatidylserine (PS) on the surface of RBC from *SOD1*^{-/-} mice that likely contribute to this observation. Indeed, under physiological conditions the exposure of PS on the RBC membrane is a signal for macrophages to recognize damaged or aged RBC [25]. A role for extravascular hemolysis in the mechanism contributing to HA is further supported *ex vivo* by the high heme content in BMDM after incubation with RBC from *SOD1*^{-/-} mice. This observation clearly indicated the increased susceptibility of *SOD1*^{-/-} RBC to be engulfed by phagocytes.

In this study, we characterize large changes in hepatic iron metabolism in old SOD1-deficient mice displaying mild but chronic HA. We first analyzed the expression of heme oxygenase-1 (HO-1), an enzyme responsible for heme catabolism in macrophages [26]. We found a substantial increase in HO-1 mRNA and protein expression in the liver of *SOD1*^{-/-} mice in comparison to the wt mice. In addition, HO-1 was found to be localized in KC, which exhibited strong Hb fluorescence from ingested RBC. In accordance with our data, increased hepatic HO-1 expression has also been reported in various hemolytic states [27,28], and in macrophages in an EP assay [15]. The role of HO-1 in systemic iron turnover has been confirmed in HO-1 deficiency [29,30]. The anemia and hepatic iron overload observed in HO-1-deficient subjects demonstrate the importance of this enzyme in recycling heme iron. On the other hand, it has been reported that potentiated HO-1 expression does not counteract tissue iron loading in acute hemolytic anemia [28,31]. We found that the moderate HA occurring in *SOD1*^{-/-} mice is associated with hepatic deposits of non-heme iron in KC. Therefore, the

increased expression of HO-1 in *SOD1*^{-/-} liver macrophages likely participates in the iron release from heme into the cytosol and its subsequent storage into ferritin deposits observed in these cells. We observed also a strong upregulation of the iron exporter Fpn in KC that have ingested RBC. The macrophage nature of Fpn positive liver cells in *SOD1*^{-/-} mice, has been also confirmed by immunofluorescent co-localization of F4/80 (widely used as a marker for mouse macrophages) with ferroportin (data not shown). Indeed, Fpn is highly expressed in tissue macrophages including KC [32-34]. Heparin (Hepc), a peptide secreted by the liver, binds to Fpn and causes its degradation [22]. We found that Hepc levels were reduced in *SOD1*^{-/-} mice. It has been proposed that the occurrence of elevated erythropoiesis is sufficient to explain the decreased expression of Hepc by an as yet unidentified erythroid regulator negatively controlling Hepc synthesis [35]. Indeed, enhanced erythropoietic activity as a compensatory reaction in HA in *SOD1*^{-/-} has been demonstrated by means of increased reticulocyte counts and splenomegaly [this study, 10]. Interestingly, expansion of the splenic erythroid pool has been reported in erythropoietin- and phenylhydrazine-treated mice [36]. In addition, Fpn expression was shown to be enhanced after EP in macrophages [15,37]. Therefore, we propose that the up-regulation of Fpn detected in KC of *SOD1*-deficient mice is the consequence of decreased Hepc level and enhanced phagocytosis of *SOD1*^{-/-} RBC. Although the coordinated down- and upregulation of Hepc and Fpn, respectively, in the liver is well-documented [38-40], its relevance for iron flux through this organ has not been clearly considered. In our mouse model of mild HA, the increased levels of hepatic Fpn protein of *SOD1*^{-/-} mice may suggest iron release from the liver and in particular from KC. In consequence, serum iron concentration is maintained at normal level despite increased iron demand for erythropoiesis. Consistent with this hypothesis, overexpression of Fpn in tissue culture cells was found to result in increased iron efflux and cellular iron depletion [32,37]. Of particular interest, overexpression of Fpn in J774 macrophages was associated with increase in the export of iron after EP [41]. Interestingly, no iron deposit was found in hepatocytes and L-ferritin, mostly expressed in these cells [42], tends to decrease in *SOD1*^{-/-} liver. However, several observations indicate that decrease of hepatic L-Ft in *SOD1*-deficient mice reflects hepatocytic secretion in response to inflammation [43] rather than iron depletion in these cells *via* upregulation of Fpn. Despite clear mRNA expression of the *Fpn1* gene in hepatocytes [44], the protein expression and its subcellular localization in these cells remain poorly documented [39]. Furthermore, in mice lacking *Hamp* gene, an upregulation of Fpn in liver did not prevent iron overload in hepatocytes whereas KC were iron deficient [39,45]. Finally, in contrast to KC we did not detect any specific labeling of Fpn in *SOD1*^{-/-} hepatocytes.

In summary, we have characterized large changes in iron and heme metabolism triggered in response to modest HA induced by oxidative stress due to *SOD1* deficiency and age-related decrease in antioxidant defense. The changes act to reduce the toxicity of Hb and/or heme released from oxidatively damaged RBC through efficient clearance of these iron compounds from circulation. In addition, combined upregulation of HO-1 and Fpn in KC of *SOD1*^{-/-} mice suggest that at least a part of heme iron is recycled into the circulation likely to respond to the needs of erythropoiesis.

ACKNOWLEDGMENTS

We would like to thank Drs. C. Bouton and J-C. Drapier (ICSN-CNRS, Gif-sur-Yvette, France) and Dr. S. Imbeaud and L. Marisa (Gif-Orsay Microarray Platform, CNRS, Gif-sur-Yvette, France) for enabling us to compare the iron-related gene expression profiles of aged *SOD1*^{-/-} vs *SOD1*^{+/+} mice by DNA microarray technology, which was helpful for designing the experiments described in this manuscript. We thank Olivier Thibaudeau for help in histological analysis. We thank John Gittins for critical reading the manuscript. This work

was supported by grant from Polish Ministry of Sciences and Higher Education [N30102431/0668].

FOOTNOTES

The abbreviations used are: BMDM, bone marrow-derived macrophages; EP, erythrophagocytosis; Fpn, ferroportin; Ft, ferritin; heme oxygenase-1; HA, hemolytic anemia; Hpcd, hepcidin; KC, Kupffer cells; PS, phosphatidylserine; RBC, red blood cells; SOD1, superoxide dismutase 1;

REFERENCES

1. Okado-Matsumoto, A., Fridovich, I. (2001) Subcellular distribution of superoxide dismutases (SOD) in rat liver: Cu,Zn-SOD in mitochondria. *J. Biol. Chem.* **276**, 38388-38393
2. Reaume, A.G., Elliott, J.L., Hoffman, E.K., Kowall, N.W., Ferrante, R.J., Siwek, D.F., Wilcox, H.M., Flood, D.G., Beal, M.F., Brown, R.H. Jr, Scott, R.W., Snider, W.D. (1996) Motor neurons in Cu/Zn superoxide dismutase-deficient mice develop normally but exhibit enhanced cell death after axonal injury. *Nat. Genet.* **13**, 43-47
3. Matzuk, M.M., Dionne, L., Guo, Q., Kumar, T.R., Lebowitz, R.M. (1998) Ovarian function in superoxide dismutase 1 and 2 knockout mice. *Endocrinology* **139**, 4008-4011
4. Sentman, M.L., Granström, M., Jakobson, H., Reaume, A., Basu, S., Marklund, S.L. (2006) Phenotypes of mice lacking extracellular superoxide dismutase and copper- and zinc-containing superoxide dismutase. *J. Biol. Chem.* **281**, 6904-6909
5. Rattan, S.I. (2006) Theories of biological aging: genes, proteins, and free radicals. *Free Radic. Res.* **40**, 1230-1238
6. Elchuri, S., Oberley, T.D., Qi, W., Eisenstein, R.S., Jackson Roberts, L., Van Remmen, H., Epstein, C.J., Huang, T.T. (2005) CuZnSOD deficiency leads to persistent and widespread oxidative damage and hepatocarcinogenesis later in life. *Oncogene* **24**, 367-380
7. Keithley, E.M., Canto, C., Zheng, Q.Y., Wang, X., Fischel-Ghodsian, N., Johnson, K.R. (2005) Cu/Zn superoxide dismutase and age-related hearing loss. *Hear Res.* **209**, 76-85
8. Muller, F.L., Song, W., Liu, Y., Chaudhuri, A., Pieke-Dahl, S., Strong, R., Huang, T.T., Epstein, C.J., Roberts, L.J. 2nd, Csete, M., Faulkner, J.A., Van Remmen, H. (2006) Absence of CuZn superoxide dismutase leads to elevated oxidative stress and acceleration of age-dependent skeletal muscle atrophy. *Free Radic. Biol. Med.* **40**, 1993-2004
9. Baumbach, G.L., Didion, S.P., Faraci, F.M. (2006) Hypertrophy of cerebral arterioles in mice deficient in expression of the gene for CuZn superoxide dismutase. *Stroke* **37**, 1850-1855
10. Iuchi, Y., Okada, F., Onuma, K., Onoda, T., Asao, H., Kobayashi, M., Fuji, J. (2007) Elevated oxidative stress in erythrocytes due to an SOD1 deficiency causes and triggers autoantibody production. *Biochem J.* **402**, 219-227
11. Hadjur, S., Ung, K., Wadsworth, L., Dimmick, J., Rajcan-Separovic, E., Scott, R.W., Buchwald, M., Jirik, F.R. (2001) Defective hematopoiesis and hepatic steatosis in mice with combined deficiencies of the genes encoding Fancd and Cu/Zn superoxide dismutase. *Blood* **98**, 10003-10011
12. Starzyński, R.R., Lipiński, P., Drapier, J-C., Diet, A., Smuda, E., Bartłomiejczyk, T., Gralak, M.A., Kruszewski, M. (2005) Down-regulation of iron regulatory protein 1 activities and expression in superoxide dismutase 1 knock-out mice is not associated with alterations in iron metabolism. *J. Biol. Chem.* **280**, 4207-4212

13. Canonne-Hergaux, F., Donovan, A., Delaby, C., Wang, H.J., Gros, P. (2006) Comparative studies of duodenal and macrophage ferroportin proteins. *Am. J. Physiol. Gastrointest. Liver Physiol.* **290**, G156–G163
14. Torrance, J.D., Bothwell, T.H. (1980) Iron stores. *Meth. Hematol.* **1**, 90-115
15. Delaby, C., Pilard, N., Hetet, G., Driss, F., Grandchamp, B., Beaumont, C., Canonne-Hergaux, F. (2005) A physiological model to study iron recycling in macrophages. *Exp. Cell Res.* **310**, 43-53
16. Motterlini, R., Foresti, R., Vandegriff, K., Intaglietta, M., Winslow, R.M. (1995) Oxidative-stress response in vascular endothelial cells exposed to a cellular hemoglobin solutions. *Am. J. Physiol.* **269**, H648-55
17. Ascenzi, P., Bocedi, A., Visca, P., Altruda, F., Tolosano, E., Beringhelli, T., Fasano, M. (2005) Hemoglobin and heme scavenging. *IUBMB Life.* **57**, 749-759
18. Kristiansen, M., Graversen, J.H., Jacobsen, C., Sonne, O., Hoffman, H.J., Law, S.K.A., Moestrup, S.K. (2001) Identification of the hemoglobin receptor. *Nature* **409**, 198-201
19. Hvidberg, V., Maniecki, M.B., Jacobsen, C., Højrup, P., Møller, H.J., Moestrup, S.K. (2005) Identification of the receptor scavenging hemopexin-heme complexes. *Blood* **106**, 2572-2579
20. Madsen, M., Møller, H.J., Nielsen, M.J., Jacobsen, C., Graversen, J.H., van den Berg, T. & Moestrup, S.K. (2004) Molecular characterization of the haptoglobin-hemoglobin receptor CD163. Ligand binding properties of the scavenger receptor cysteine-rich domain region. *J. Biol. Chem.* **279**, 51561-51567.
21. Dhaliwal, G., Cornett, P.A., Tierney, L.M. Jr. (2004) Hemolytic anemia. *Am. Fam. Physician* **69**, 2599-2606
22. De Domenico, I., Ward, D.M., Langelier, C., Vaughn, M.B., Nemeth, E., Sundquist, W.I., Ganz, T., Musci, G., Kaplan, J. (2007) The molecular mechanism of hepcidin-mediated ferroportin down-regulation. *Mol. Biol. Cell.* **18**, 2569-2578
23. Kumar, S., Bandyopadhyay, U. (2005) Free heme toxicity and its detoxification systems in human. *Toxicol. Lett.* **157**, 175-188
24. Delanghe, J.R., Langlois, M.R. (2001) Hemopexin: a review of biological aspects and the role in laboratory medicine. *Clin. Chim Acta* **312**, 13-23
25. Bratosin, D., Mazurier, J., Tissier, J.P., Estaquier, J., Huart, J.J., Ameisen, J.C., Aminoff, D., Montreuil, J. (1998) Cellular and molecular mechanisms of senescent erythrocyte phagocytosis by macrophages. *Biochimie* **80**, 173-195
26. Maines, M.D. (2005) The heme oxygenase system: update 2005. *Antioxid. Redox Signal.* **7**, 1761-1766.
27. Immenschuh, S., Shan, Y., Kroll, H., Santoso, S., Wössmann, W., Bein, G., Bonkovsky, H.L. (2007) Marked hyperbilirubinemia associated with the heme oxygenase-1 gene promoter microsatellite polymorphism in a boy with autoimmune hemolytic anemia. *Pediatrics* **119**, e764-767
28. Tolosano, E., Fagoonee, S., Hirsch, E., Berger, F.G., Baumann, H., Silengo, L., Altruda, F. (2002) Enhanced splenomegaly and severe liver inflammation in haptoglobin/hemopexin double-null mice after acute hemolysis. *Blood* **100**, 4201-4208
29. Poss, K.D., Tonegawa, S. (1997) Heme oxygenase 1 is required for mammalian iron utilization. *Proc. Natl. Acad. Sci USA* **94**, 10919-10924
30. Yachie, A., Niida, Y., Wada, T., Igarashi, N., Kaneda, H., Toma, T., Ohta, K., Kasahara, Y., Koizumi, S. (1999) Oxidative stress causes enhanced endothelial cell injury in human heme oxygenase-1 deficiency. *J. Clin. Invest.* **103**, 129-135
31. Khan, Z.A., Barbin, Y.P., Cukiernik, M., Adams, P.C., Chakrabarti, S. (2004) Heme-oxygenase-mediated iron accumulation in the liver. *Can. J. Physiol. Pharmacol.* **82**, 448-456

32. Abboud, S., Haile, D.J. (2000) A novel mammalian iron-regulated protein involved in intracellular iron metabolism. *J. Biol. Chem.* **275**, 19906-19912
33. McKie, A.T., Marciani, P., Rolfs, A., Brennan, K., Wehr, K., Barrow, D., Miret, S., Bomford, A., Peters, T.J., Farzaneh, F., Hediger, M.A., Hentze, M.W., Simpson, R.J. (2000) A novel duodenal iron-regulated transporter, IREG1, implicated in the basolateral transfer of iron to the circulation. *Mol. Cell.* **5**, 299-309
34. Donovan, A., Brownlie, A., Zhou, Y., Shepard, J., Pratt, S.J., Moynihan, J., Paw, B.H., Drejer, A., Barut, B., Zapata, A., Law, T.C., Brugnara, C., Lux, S.E., Pinkus, G.S., Pinkus, J.L., Kingsley, P.D., Palis, J., Fleming, M.D., Andrews, N.C., Zon, L.I. (2000) Positional cloning of zebrafish ferroportin1 identifies a conserved vertebrate iron exporter. *Nature* **403**, 776-781
35. Vokurka, M., Krijt, J., Sulc, K., Necas, E. (2006) Hepcidin mRNA levels in mouse liver respond to inhibition of erythropoiesis. *Physiol. Res.* **55**, 667-674
36. Canonne-Hergaux, F., Zhang, A.S., Ponka, P., Gros, P. (2001) Characterization of the iron transporter DMT1 (NRAMP2/DCT1) in red blood cells of normal and anemic mk/mk mice. *Blood* **98**, 3823-3830
37. Knutson, M.D., Vafa, M.R., Haile, D.J., Wessling-Resnick, M. (2003) Iron loading and erythrophagocytosis increase ferroportin 1 (FPN1) expression in J774 macrophages. *Blood* **102**, 4191-4197
38. Delaby, C., Pilard, N., Gonçalves, A.S., Beaumont, C., Canonne-Hergaux, F. (2005) Presence of the exporter ferroportin at the plasma membrane of macrophages is enhanced by iron loading and down-regulated by hepcidin. *Blood* **106**, 3979-3984.
39. Viatte, L., Lesbordes-Brion, J.C., Lou, D.Q., Bennoun, M., Nicolas, G., Kahn, A., Canonne-Hergaux, F., Vaulont, S. (2005) Deregulation of proteins involved in iron metabolism in hepcidin-deficient mice. *Blood* **105**, 4861-4864.
40. Peyssonnaud, C., Zinkernagel, A.S., Schuepbach, R.A., Rankin, E., Vaulont, S., Haase, V.H., Nizet, V., Johnson, R.S. (2007) Regulation of iron homeostasis by the hypoxia-inducible transcription factors (HIFs). *J. Clin. Invest.* **117**, 1926-1932
41. Knutson, M.D., Oukka, M., Koss, L.M., Aydemir, F., Wessling-Resnick, M. (2005) Iron release from macrophages after erythrophagocytosis is up-regulated by ferroportin 1 overexpression and down-regulated by hepcidin. *Proc. Natl. Acad. Sci. USA.* **102**, 1324-1328
42. Doolittle, R.L., Richter, G.W. (1981) Isoferritins in rat Kupffer cells, hepatocytes, and extrahepatic macrophages. Biosynthesis in cell suspensions and cultures in response to iron. *Lab. Invest.* **45**, 567-574
43. Tran, T.N., Eubanks, S.K., Schaffer, K.J., Zhou, C.Y.J., Linder, M.C. (1997) Secretion of ferritin by rat hepatoma cells and its regulation by inflammatory cytokines and iron. *Blood* **12**, 4979-4986
44. Zhang, A.S., Xiong, S., Tsukamoto, H., Enns, C.A. (2004) Localization of iron metabolism-related mRNAs in rat liver indicate that HFE is expressed predominantly in hepatocytes. *Blood* **103**, 1509-1514.
45. Nicolas, G., Bennoun, M., Devaux, I., Beaumont, C., Grandchamp, B., Kahn, A., Vaulont, S. (2001) Lack of hepcidin gene expression and severe tissue iron overload in upstream stimulatory factor 2 (USF2) knockout mice. *Proc. Natl. Acad. Sci. USA.* **98**, 8780-8785

FIGURE LEGENDS

Table 1 Changes in the hematological parameters of 1-year-old *SOD1*^{-/-} mice. Values are expressed as the mean \pm SD. Blood cell indices were determined for 10 mice of each genotype. RBC, red blood cells number; Hb, hemoglobin; HCT, hematocrit; MCV, mean cell volume, MCH, mean cell hemoglobin; MCHC, mean cell hemoglobin concentration. * denotes significant differences between *SOD1*^{-/-} and *SOD1*^{+/+} mice, $P < 0.05$.

Figure 1 Evidence of regenerative and not associated with iron deficiency anemia in *SOD1*^{-/-} mice. (A) Increased number of reticulocytes in peripheral blood of *SOD1*^{-/-} mice. (B) Increased spleen index in *SOD1*^{-/-} mice. Spleen index (SI) was calculated according to the formula $SI = \sqrt{100 * spleen_weight / body_weight}$ [45]. (C) Serum iron and (D) serum transferrin levels in *SOD1*^{-/-} and *SOD1*^{+/+} mice, N=8-10 for each genotype. * Denotes significant differences between values for *SOD1*^{-/-} and *SOD1*^{+/+} mice, ($P < 0.05$).

Figure 2 Changes in the expression of haptoglobin (Hp), hemopexin (Hx) and their receptors in *SOD1*^{-/-} mice. (A) Plasma levels of Hp and Hx were assessed by Western blotting. For Hp detection, proteins from 1 μ l of plasma were separated by SDS-polyacrylamide gel electrophoresis. For detection of Hx, 2 μ l of plasma was diluted in 40 μ l of loading buffer and then 5 μ l was loaded on a SDS-polyacrylamide gel. Plasma from LPS-treated *SOD1*^{+/+} mice and from Hx-null mice (kindly provided by Dr. E. Tolosano, University of Turin) were used as positive and negative controls, respectively. Red Ponceau staining of transferred proteins is shown (lower panels) to confirm equivalent loading. (B) Hepatic Hp and Hx mRNA levels. Transcript abundance in livers was measured by Real-Time RT-PCR using specific primer pairs shown in supplementary data (Fig 1). Each column represents the mean \pm S.D. of two amplification reactions, performed using a single cDNA sample reverse-transcribed from RNA prepared from four mice of each genotype. To confirm amplification specificity, the PCR products from each primer pair were subjected to melting curve analysis and subsequent agarose gel electrophoresis. The levels of Hp and Hx mRNA in *SOD1*^{+/+} mice were assigned as the 100% values. N=4, ($P < 0.05$). (C) Hepatic CD163 and CD91 mRNA levels measured by Real-Time RT-PCR. For description see B.

Figure 3 Indices of increased extravascular hemolysis in *SOD1*-deficient mice. (A) Increased externalization of phosphatidylserine (PS) on *SOD1*^{-/-} erythrocytes. Exposure of PS was assessed by staining cells with Annexin V-FITC followed by flow cytometry. Artificially-aged, Ca²⁺ ionophore A23187-treated RBCs from *SOD1*^{+/+} mice were used as control cells showing high levels of PS exposure on their cell membrane. Stained RBC as a percentage of the total number of erythrocytes was calculated. Results are shown as the mean \pm SD for 3 wild-type mice and 4 *SOD1*^{-/-} mice. Significant differences in PS exposure are indicated. (B) Increased heme content of bone marrow-derived macrophages (BMDM) after *in vitro* phagocytosis of erythrocytes. The erythrophagocytosis assay was performed using BMDM from *SOD1*^{+/+} mice and red blood cells (RBC) from 1-year-old *SOD1*^{-/-} and *SOD1*^{+/+} mice. Heme content of the formic acid-solubilized BMDM was determined spectrophotometrically at 398 nm. Values represent the means \pm SD of 4 erythrophagocytosis assays performed in duplicate on RBC from 4 mice of each genotype. Significant differences in PS exposure are indicated. ($P < 0.05$).

Figure 4 Increased hepatic heme oxygenase-1 (HO-1) expression in *SOD1*^{-/-} mice. (A) Hepatic HO-1 mRNA level. Transcript abundance in livers was measured by real-time RT-PCR using the specific primer pair shown in supplementary data (Table 1). Reactions and data

presentation, as described in the legend to Fig 1B. **(B)** HO-1 protein levels as assessed by Western blotting. Membrane proteins from liver (100 μ g/lane) were separated by SDS-polyacrylamide gel electrophoresis. An identical blot reacted with actin antibody is shown (lower panel) to confirm equivalent loading. **(C)** Immunofluorescence staining of HO-1 and **(D)** autofluorescence of hemoglobin in *SOD1*^{-/-} (-/-) and *SOD1*^{+/+} (+/+) livers analyzed by fluorescence microscopy (original magnification 60x). **(E)** Enlargements of fluorescent staining in *SOD1*^{-/-} liver show HO-1 expression in hemoglobin-containing Kupffer cells.

Figure 5 Hepatic iron status in *SOD1*^{-/-} mice and wild-type littermates. **(A)** Histological examination of iron loading in liver. Non-heme iron deposits were detected by staining with Perls Prussian blue (blue stain) exclusively in Kupffer cells of *SOD1*^{-/-} mice (arrows). A high magnification of a Kupffer cells presenting clear deposit of iron likely in ferritin is shown (inset in the bottom right panel). **(B)** Non-heme hepatic iron content was measured as described under Experimental. Values are expressed as the mean \pm SD for liver samples obtained from 10 mice of each genotype, ($P < 0.05$). **(C)** H- and L-ferritin levels in liver cytosolic protein extracts (50 μ g/lane) were assessed by Western Blotting. The analyses were performed in quadruplicate using extracts obtained from different *SOD1*^{-/-} and *SOD1*^{+/+} mice, and representative results are shown.

Figure 6 Correlation between enhanced ferroportin (Fpn) and decreased hepcidin expression in the liver of *SOD1*^{-/-} mice. **(A)** Ferroportin levels in liver membrane protein extracts (100 μ g/lane) as assessed by Western blotting. Red Ponceau staining of transferred proteins and an identical blot reacted with actin antibody are shown (lower panels) to confirm equivalent loading. **(B)** Immunofluorescence staining of Fpn and RBC (hemoglobin autofluorescence) in liver sections from *SOD1*^{-/-} and *SOD1*^{+/+} mice (original magnification 63x). Lower panels show enlargement of Fpn staining in Kupffer cells of wild-type (+/+) or *SOD1*-deficient (-/-) mice. In *SOD1*^{-/-} mice Fpn was detected in liver macrophages containing RBC. **(C)** Expression of ferroportin mRNA. Transcript abundance in livers of *SOD1*^{-/-} and *SOD1*^{+/+} mice was measured by real-time RT-PCR using the specific primer pair shown in supplementary data (Table 1). Reactions and data presentation, as described in the legend to Fig 2B. **(D)** Expression of hepcidin mRNA. Transcript abundance in livers of *SOD1*^{-/-} and *SOD1*^{+/+} mice was measured by real-time RT-PCR using the specific primer pair shown in supplementary data Table 1). Reactions and data analysis as described in the legend to Fig 2B, except that six mice of each genotype were used. * Denotes significant differences between hepcidin mRNA levels in the livers of *SOD1*^{-/-} and *SOD1*^{+/+} mice ($P < 0.05$).

Table 1 Changes in the hematological parameters of 1-year-old *Sod1*^{-/-} mice

genotype	RBC <i>10</i> ⁶ / <i>μ</i> L	Hb g/dL	HCT %	MCV fL	MCH pg	MCHC g/dL
<i>SODI</i> ^{+/+}	7.2 ± 0.6	12.5 ± 1.1	39.1 ± 3.9	54.3 ± 1.6	17.5 ± 0.4	32.2 ± 1.5
<i>SODI</i> ^{-/-}	5.5 ± 0.5*	9.8 ± 0.9*	32.1 ± 3.5*	58.0 ± 2.5*	17.8 ± 0.3	30.7 ± 0.9

Values are expressed as the mean ± SD. Blood cell indices were determined for 10 mice of each genotype. RBC, red blood cells number; Hb, hemoglobin; HCT, hematocrit; MCV, mean cell volume, MCH, mean cell hemoglobin; MCHC, mean cell hemoglobin concentration. * denotes significant differences between *Sod1*^{-/-} and *Sod1*^{+/+} mice, *P* < 0.05.

Figure 1

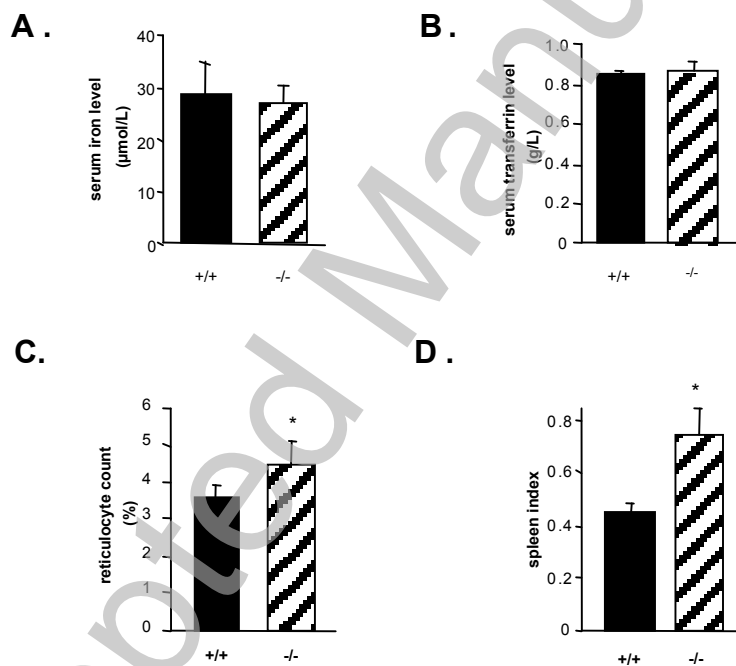
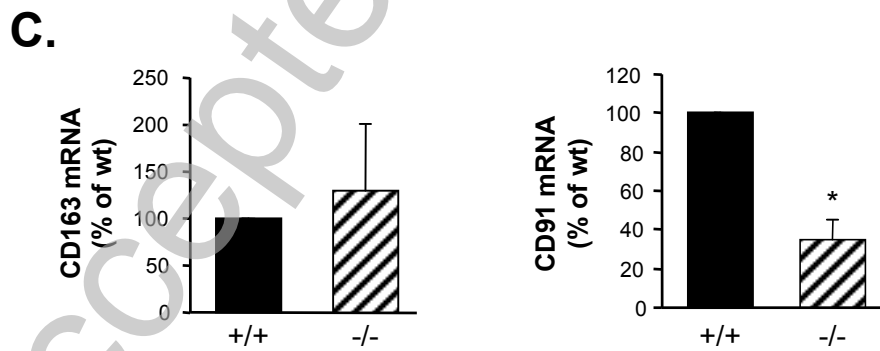
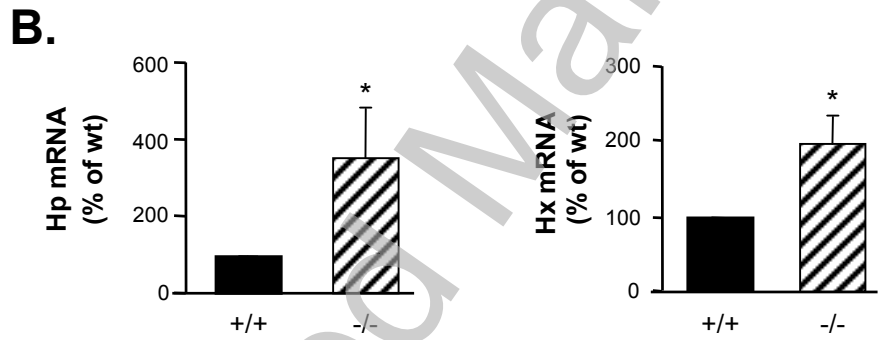
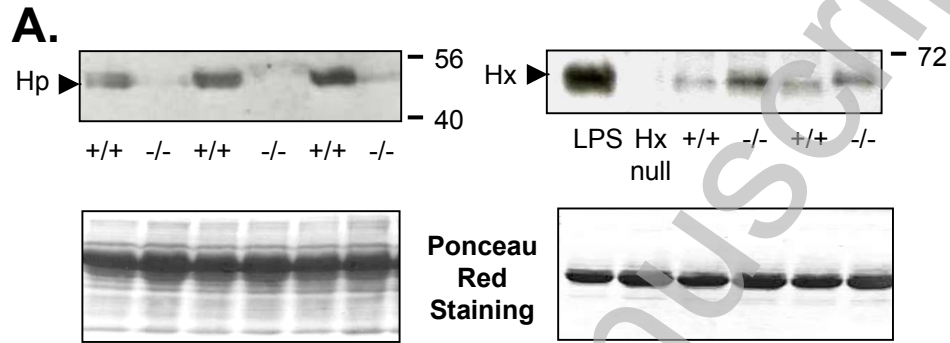


Figure 2



THIS IS NOT THE VERSION OF RECORD - see doi:10.1042/BJ20082137

Figure 3

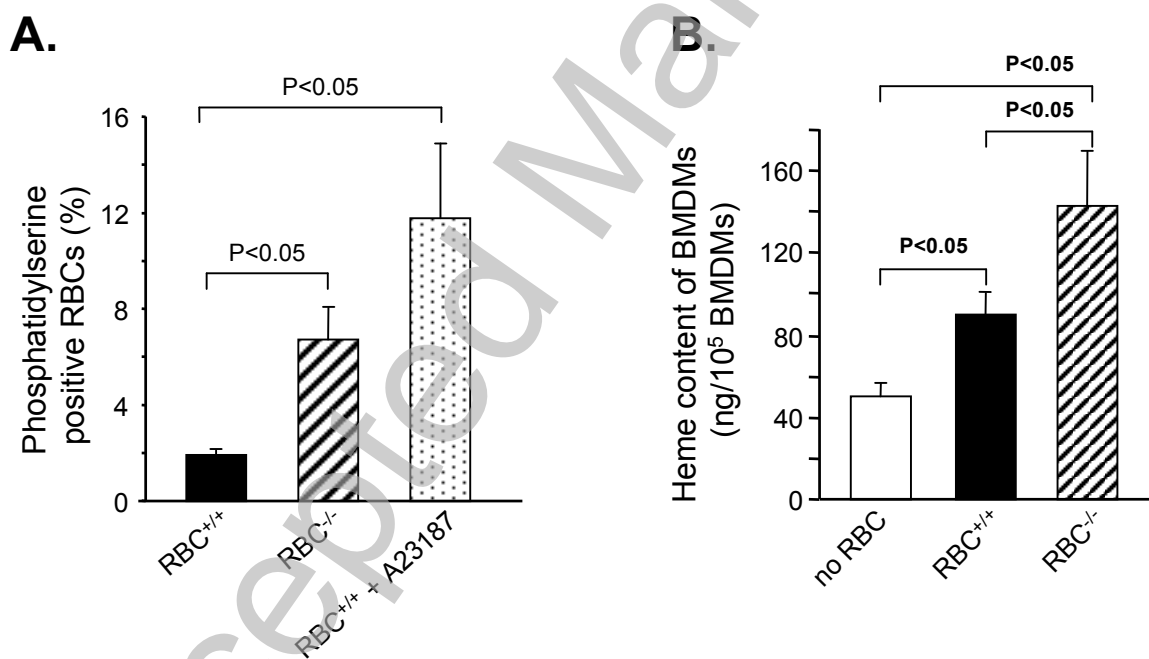
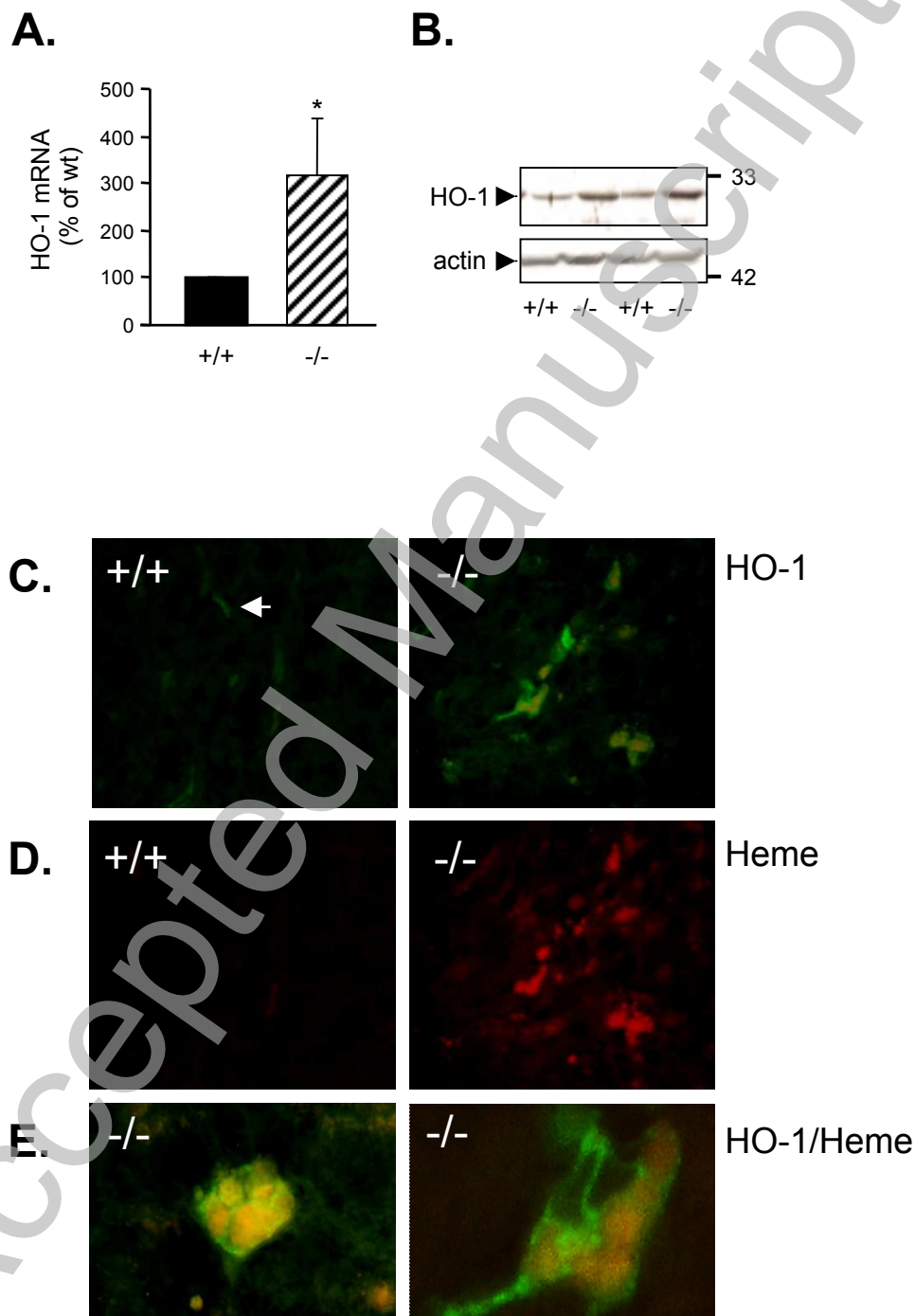
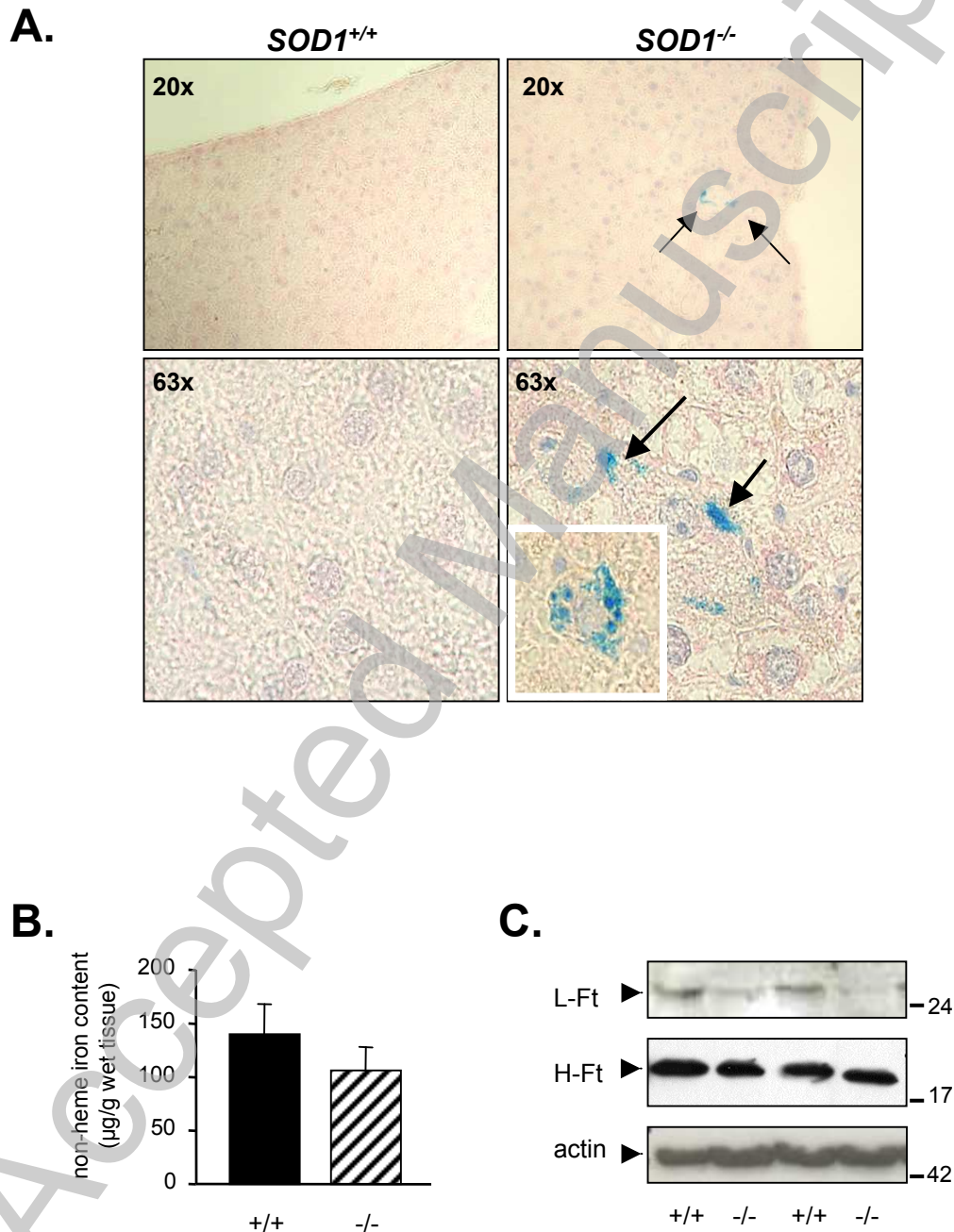


Figure 4



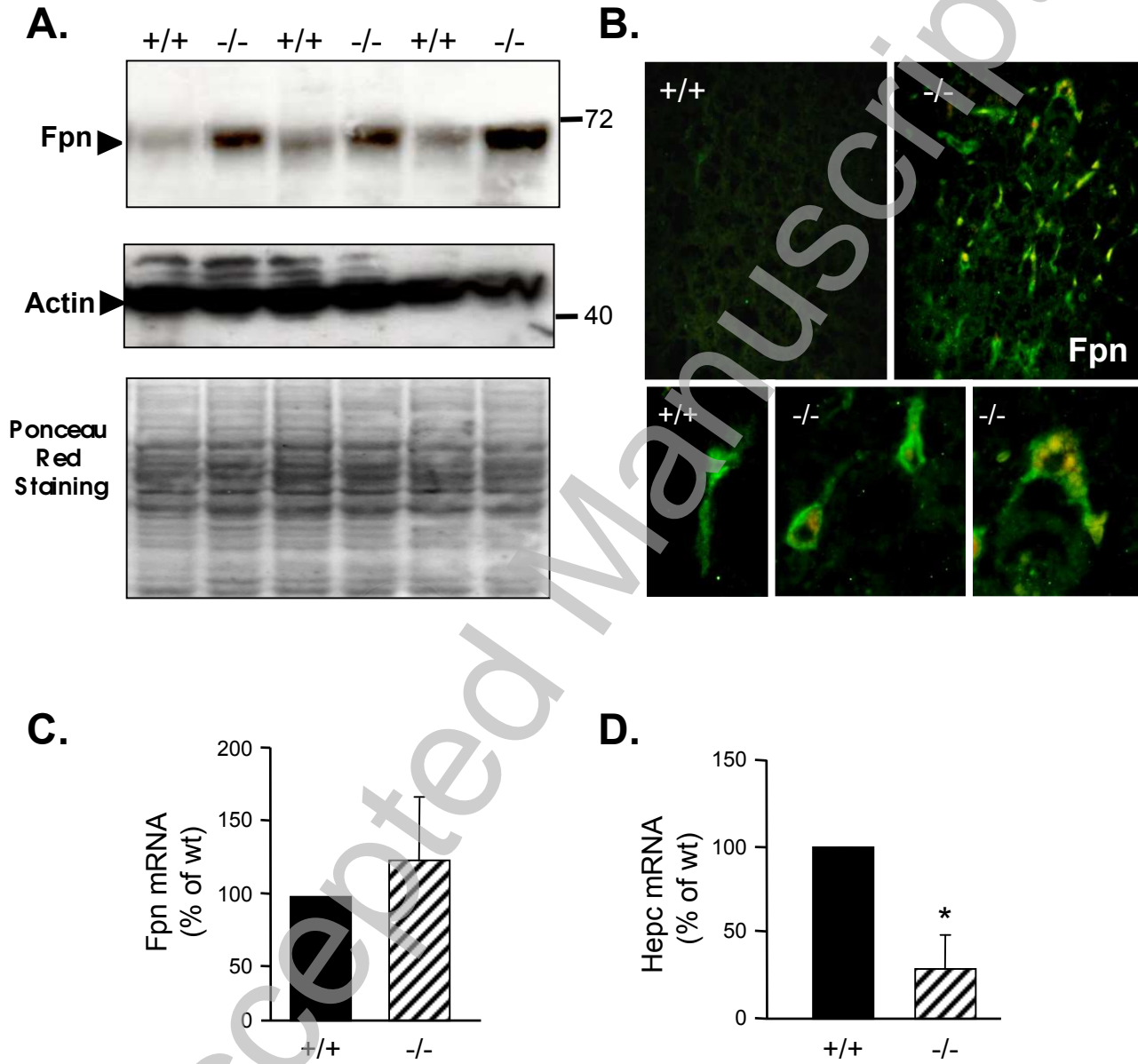
THIS IS NOT THE VERSION OF RECORD - see doi:10.1042/BJ20082137

Figure 5



THIS IS NOT THE VERSION OF RECORD - see doi:10.1042/BJ20082137

Figure 6



THIS IS NOT THE VERSION OF RECORD - see doi:10.1042/BJ20082137